CHEMICAL ENGINEERING TRANSACTIONS
VOL. 88, 2021
A publication of AIDIC
The Italian Association of Chemical Engineering
Online at www.cetjournal.it
Guest Editors: Petar S. Varbanov, Yee Van Fan, Jiří J. Klemeš

ISBN 978-88-95608-86-0; **ISSN** 2283-9216
DOI: 10.3303/CET2188024

Cryogenic Removal of CO_2 by Frost Formation from Biogas

Sylvain Haddad, Rodrigo Rivera-Tinoco, Chakib Bouallou*

MINES Paris – PSL Université Paris, Center for Energy Efficiency of Systems, 5 rue Léon Blum 91120 Palaiseau, France
chakib.bouallou@mines-paristech.fr

Removal of carbon dioxide to upgrading biogas is possible by cryogenics and frost formation. In this work, it is targeted removing carbon dioxide by frost deposition (physical transition from gas to solid state) at low pressure and temperature from biogas, as well as assessing the impact of mass flow rate, temperature and the initial CO_2 content in biogas on the carbon dioxide removal process. The Solid-Gas phase equilibrium between CH_4 and CO_2 is presented. It is followed by a sensitivity study of CO_2 deposition on a flat plate and the assessment of different geometries of the heat exchanger generating frost. The global process including CO_2 removal and biomethane liquefaction is simulated in AspenTech tools that are linked to a specific module modelling frost formation phenomenon. This module is coded in Dymola (Modelica language). Different operating modes of the heat exchanger are compared: thermal inertia or by direct cooling by nitrogen gas obtained after liquefaction of the biomethane. The temperature of the heat exchanger increases as CO_2 deposits. Results show that cryogenic CO_2 frost formation can be used for simultaneous liquefaction and upgrading of methane at 97% vol. minimum of purity and a reduction of cooling cycles on site by cold recovery from frost. This implies a reduction of energy intensity to remove carbon dioxide compared to conventional cryogenic technologies.

1. Introduction

One of the solutions to reduce greenhouse gas emissions from fossil fuels is the use of biogas that is originated from biomass decomposition (Martin and Murach, 2012). In 2018, the top ten European countries in terms of biogas production accounted for 38.9 % of global production, followed by China and the United States, 31.25 % and 24.73 %, respectively (MRR, 2018). In the coming years, demand of biogas is expected to continuously increase as governments are reinforcing policy towards renewable energy supply, following the example of countries like Sweden, France, Germany and the Netherlands, that are already producing methane from biogas at industrial scale (Chaemchuen et al., 2013). The removal of some pollutants and intert gases from the biogas is compulsory to prevent premature damage of equipment and proper performance of systems. H_2S removal from biogas enables its direct use in Combined Heat and Power units (CHP), either engines or turbines, and boilers, whereas the injection of biogas to gas grids or the use in vehicles as fuel requires a high purity of methane, hence also the removal of CO_2 (Wilken et al., 2017).
Among several mature technologies for carbon dioxide removal from several gases, cryogenic technologies have been studied for years with little market penetration. In 2012, Xu et al. (2012) proposed a two-stage compression-refrigeration process to remove CO_2 from H_2. The higher pressure of the mixture, prior to the separation of CO_2, reduces the need for cooling at low temperatures. However, compressor costs hampered the deployment. Other processes of CO_2 removal by cryogenic processes are found in the treatment of exhaust gases from power plants. According to Clodic and Younes (2003), the deposition temperature of CO_2 depends on its partial pressure in the mixture and the interaction within the chemical species in the gas phase. The system studied consists of a batch heat exchanger collecting frost while a second heat exchanger melts/sublimate the frost to prepare the frost formation again. Tuinier et al. (2011). proposed a “cryogenic packed bed” and appeared as a solution for clogging problems encountered in the batch heat exchangers presented in previous works. When the bed temperature is unable to lead the gas stream to the expected CO_2 concentration, either the packed bed circulates or it begins a regeneration phase. Song et al. (2012) proposed a post-combustion cryogenic CO_2 capture process using Stirling machines, mentioning high efficiency, high reliability

Paper Received: 23 May 2021; Revised: 22 September 2021; Accepted: 4 October 2021
Please cite this article as: Haddad S., Rivera-Tinoco R., Bouallou C., 2021, Cryogenic Removal of CO_2 by Frost Formation from Biogas, Chemical Engineering Transactions, 88, 145-150 DOI:10.3303/CET2188024

and small size. Cryogenics has several advantages, among them the avoidance of chemicals and the capability to operate in a wide range of pressures.
This work focuses on biogas upgrading no data can be found concerning biogas upgrading using cryogenic processes. Potential use is very relevant, as cryogenics can enable a biomethane purity of 99 % with low methane losses (1 %) (Kadam and Panwar, 2017). Moreover, this work includes the use of nitrogen as liquefaction media for biomethane produce, which leads to the availability of nitrogen to evaporate CO_2 to recover cold from the frost obtained.

2. CO_2-CH_4 in solid phase and modelling of frost formation

2.1 Phase equilibrium

When studying frost formation, CO_2 concentration in the near-surface of the heat exchanger and the gas stream is related to the surface temperature (the boundary layer temperature) by the psychrometric diagram. Specific psychrometric diagrams for CH_4/CO_2 were constructed. Similarly, by analogy to water-air oneby following the methodology of He Sheng Ren (2004). Humid air is replaced with biogas, CH_4 represents the dry air and CO_2 the water vapour. The saturation P-T values are obtained and using a curve fitting program of Refprop V9.1.

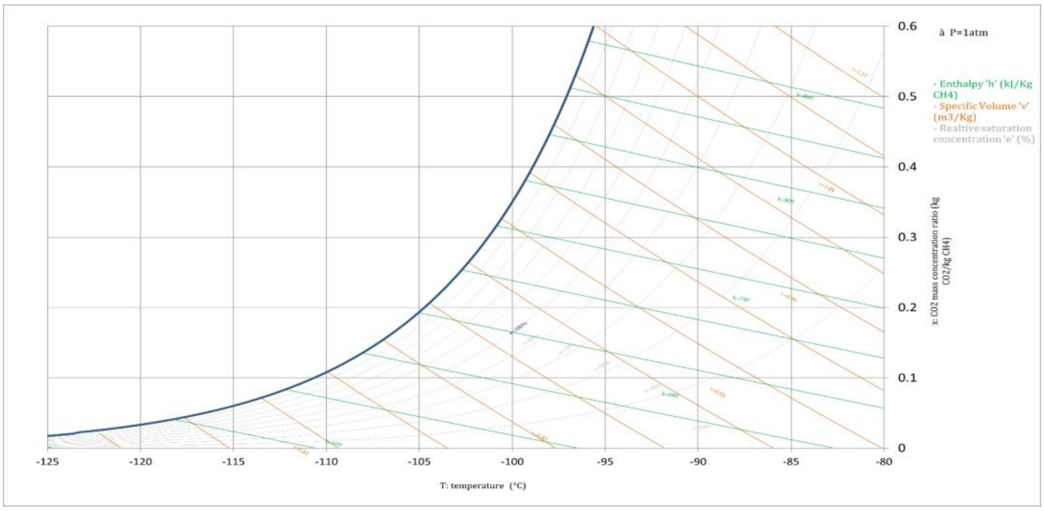

Figure 1: Psychrometric chart for CH_4/CO_2 with temperature and concentration evolution in frosting conditions (Haddad, 2019)

2.2 Modelling

In Figure 2 it is schematized the heat and mass transfer phenomena occurring during frost formations. The gas entering a cold heat exchanger from the left is cooled down. The driving force is the saturation (concentration) and temperature of CO_2 in the gas phase and the cold surface-gas stream, respectively. The layer of frost increases and heat is hence transferred by conduction from the cold surface of the heat exchanger to the gas phase. CO_2 keeps condensing inside the pores of the frost layer and in the surface, making frost densification and thickening to increase.

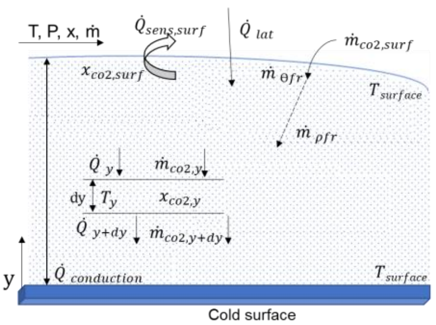

Figure 2: Energy and mass transfer on the surface and inside the frost during deposition (Haddad, 2019)

Mass and heat transfer equations are for the gas phase are:

- convection heat transfer between the gases and the cold frost surface

$$\dot{Q}_{sens} = h_c \times (T_{biogas} - T_{fr,surf}) \quad (1)$$

- frost formation CO_2 mass flux $\dot{m}_{co2,frost}$ expressed by the analogy between heat and mass transfer

$$\dot{m}_{co2,frost} = h_m \times \rho_{biogas} \times (x_{CO2/CH4} - x_{fr,surf}) \quad (2)$$

On the frost surface, the mass flow of condensed CO_2 is represented by two terms. The first is the mass flux $\dot{m}_{\rho,frost}$ which corresponds to the mass of CO_2 diffused from the surface inside the frost:

$$\dot{m}_{\rho frost,surf} = D_{eff} \times \rho_{biogas} \times (\frac{dx_{biogas}}{dy})_{y=y,surf} \quad (3)$$

And the second $\dot{m}_{\theta,frost}$ corresponds to the condensation of CO_2 on the frost surface which increases its thickness.

$$\frac{d\theta_{frost}}{dt} = \dot{m}_{\theta frost}/\rho_{frost} \quad (4)$$

The total heat transfer at the frost surface is described by the following equations:

$$\dot{Q}_{tot,surf} = \dot{q}_{sens} + \dot{q}_{lat,surf} \quad (5)$$

$$\dot{Q}_{lat,surf} = \dot{m}_{\theta frost} \times L_{sv} \quad (6)$$

$$\dot{Q}_{cond,surf} = k_{frost} \times (\frac{dT_{fr}}{dy})_{y=y,surf} \quad (7)$$

In which $(\frac{dT_{fr}}{dy})_{y=y,surf}$ represents the temperature gradient between the frost layers when y tends to θ_{frost}, that is to say on the surface of the frost. Inside the frost layer, frosted CO_2 mass flow is obtained by the law of Fick for the diffusion of matte, considering that the effective diffusion coefficient D_{eff} is limited by the porosity of the CO_2 frost layer, according to Lee et al. (1997).

3. Results

3.1 Reference case

In this part is conducted a first simulation of a frost heat exchanger to understand the effect of inlet conditions on the frost thickness and density evolution, as well as mass and energy balances. Biogas (CH_4-CO_2) passes over a cold plate (30 cm x 15 cm). CO_2 condenses generating frost on the mentioned surface. The operating pressure is atmospheric, very similar to the one of biogas exiting the digesters. In Table 1 are shown the different CO_2 mass concentration values of biogas inlet and temperatures considered for the sensitivity study.

Table 1: Operating conditions for reference case with CO_2 content variation

	Case 1	Case 2	Case 3
CO_2 content (kg CO_2/kg biogas)	0.4	0.5	0.6
Biogas temperature inlet at frost heat exchanger (°C)	-80	-80	-80
Temperature of the cold plate (°C)	-128	-128	-128

In part Figure 3, frost thickness will be compared for the three different values given. CO_2 inlet concentration impacts mainly the mass flux frost formation. The difference between these two values gives the mass flux of CO2 frosted at the surface will increase for a higher concentration (20 % above the reference concentration) increasing with it the frost thickness by about 13.5 %. Heat exchange surface is considered constant in this study, however, it should be highlighted that the pores increase dynamically the surface of heat and mass transfer. The frost density is calculated by considering the mass deposition by diffusion of CO_2 in the solid layers. Although an increase in the frost density reduces the thickness growth, the effect of a higher concentration on the mass flow of CO_2 frosted is more important. Frost growth creates a thermal resistance between the plate and the biogas, therefore the frost thickness and density both have lower increase slopes as more frost is formed on the plate as a function on time.

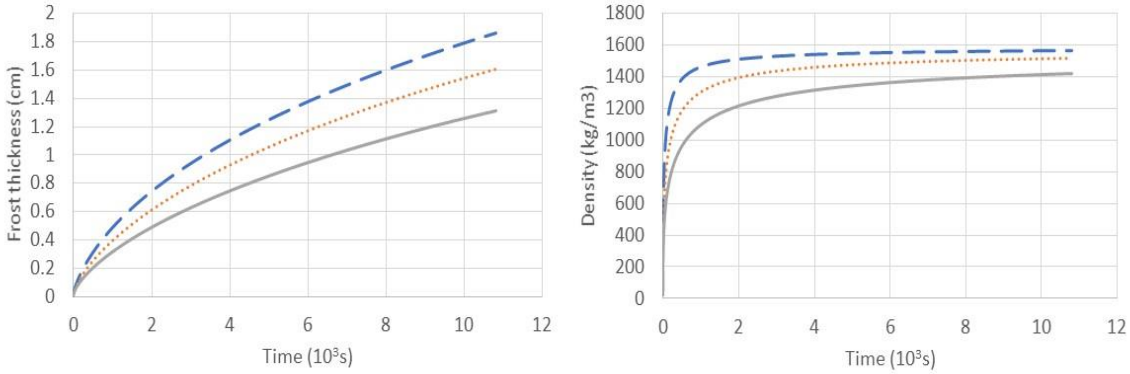

Figure 3: CO_2 frost growth for different mass concentration (Case 1 grey line, Case 2 dotted line, Case 3 dashed line), (left) frost thickness, (right) frost density

3.2 Case studies

Flat plate heat exchangers are frequently considered for studies of frost formation. However, the surface per volume ratio, as well as the homogeneity of the gas velocity in the surface are difficult to translate into applicable industrial scaled-up processes. Hence, this work aims at assessing the impact of geometry on the removal of CO_2 from biogas and on keeping the longer time possible the methane concentration constraint.

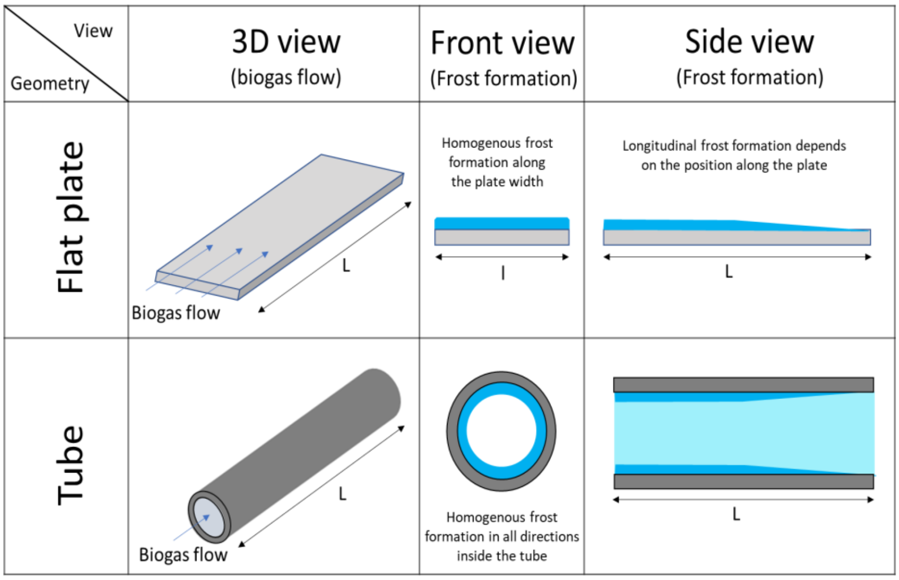

Figure 4: Geometries of frost heat exchangers considered to remove CO_2 from biogas

Molar concentration of CO_2 in biogas is frequently within a range of 20 % to 50 %. Calculations are carried out for a flow of 250 Nm^3/h of biomethane. The plate and tube heat exchanger configurations are compared for different CO_2 molar concentration and upgraded biomethane outlet flowrate, as well as on the performance of purity of methane produced. The biogas flow is dispatched in 240 tubes, of 0.02 m inner diameter with an initial temperature of -120 °C. An equivalent surface is considered for the plate and correlations for heat transferred are selected according to the geometry, either tube or plate respectively. In Figure 5 is presented the composition of methane exiting the plates or tubes respectively. A reference minimum purity value is set at 97.5 % of methane, which is the limit stated by law for biomethane purity for injection into the gas grid. In this Figure 5 results are also presented as a function of the initial molar concentration of CO_2 in the biogas, ranging from

20 % to 35 %. Results show that lower CO_2 concentrations yield to a higher CH_4 purity for longer periods of time and as frost accumulates the decrease of CH_4 outlet concentration is observed. As frosting time increases, the rate of outlet CH_4 concentration decreases at slower rate for the plate compared to the tube. At time t = 2950 s, CH_4 concentration is higher for the plate than the tube for y_co2 = 35 % (grey and green lines respectively). The CH_4 concentration curves for tube geometry seem to decrease at a higher rate than the plates. This is due to the change of the effective heat transfer area and transfer phenomena. Comparing the overall results of the tube and plate configurations, the curves show higher methane purity in tubes. Plates with same heat exchange surface are unable to satisfy the specifications on methane content of y_ch4 > 97.5 %.

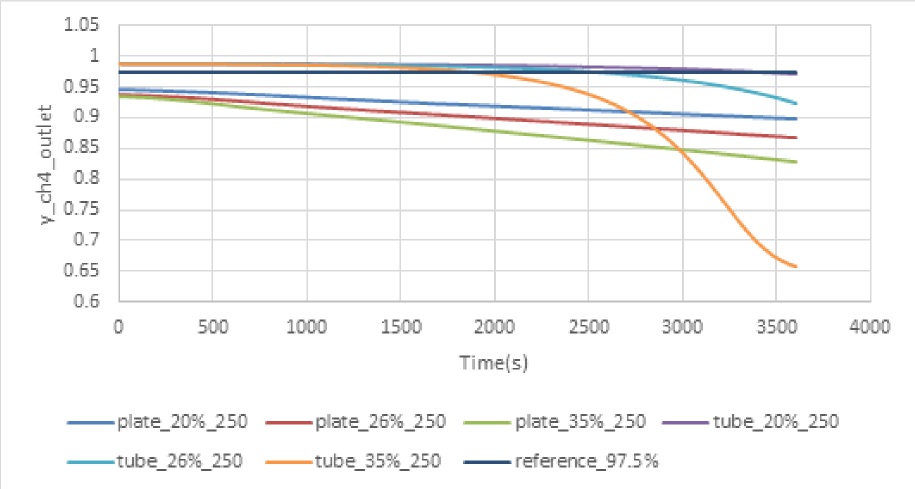

Figure 5: Outlet CH_4 concentration for different inlet CO_2 concentrations and different geometries

This confirms the suitability of tubes for collecting CO_2 from biogas and the possibility to use semibatch systems to be able to eliminate frost while a set of tubes simultaneously upgrade biomethane. One challenge that remains is the energy intensity and the cold recovery. In another work, a similar approach of frosting is considered, however it is nitrogen that evaporates the frosted CO_2 and enables cold recovery.

4. Conclusions

A sensitivity study was led on CO_2 frosting from biogas, and results show that for higher CO_2 concentrations, frost grows faster and more in terms of thickness and density. On the other hand, results for CO_2 frosting from biogas showed how higher relative concentrations of CO_2 increase heat transfer especially at the interface between the frost and the gas flow. Plate temperature has a “more constant variation” effect on heat transfer than CO_2 concentration and inlet temperature has an opposite effect than the concentration. A comparison between the plate and the tube configuration for CO_2 deposition showed that the tube presents a better configuration in terms of accessibility and heat transfer for a given time but for longer frosting periods the plate is the better choice since its heat exchange surface remains constant during CO_2 deposition. A condition on CH_4 outlet concentration is fixed at 97.5%, which represents the minimum purity to biomethane injection into the gas grid in France. The results show that frost deposition presents a certain delay along the tube; this is caused by the concentration gradient decrease as frost deposits at earlier positions in the tube. A whole system of biogas upgrading using nitrogen for liquefaction of biomethane is suggested. Gas phase obtained of nitrogen is used to sublimate from frost by an inverse phenomenon than frost formation: controlled vaporisation of solid phase and simultaneously reduce the temperature cycling of frosting plates.

Nomenclature

D_{eff} – Effective diffusion coefficient, m².s^{-1}
dt – time step, s
dx_{biogas} – differential CO_2 composition in the gas phase at position x, -
dy – differential position y, -
$d\theta_{frost}$ –thickness frost variation, m
h_c – heat transfer coefficient, kW.m^{-2}.C^{-1}
h_m – mass transfer coefficient, m.s^{-1}
k_{frost} – frost conductivity, kW.m^{-2}.C^{-1}
L – length, m
l – width, m
L_{SV} – latent heat of sublimation of CO_2, kJ.kg^{-1}
$m_{CO2,frost}$ – mass flux of CO_2 from gas phase to total frost, kg.s^{-1}.m^{-2}
$m_{CO2,surf}$ – total mass flux of CO_2 from the gas phase, kg.s^{-1}.m^{-2}

$m_{CO2,y}$ – mass flux of CO_2 in position y, $kg.s^{-1}.m^{-2}$
$m_{CO2,y+dy}$ – mass flux of CO_2 in y, $kg.s^{-1}.m^{-2}$
$m_{\theta frost}$ – mass flux of CO_2 from the gas phase contributing to thickness increase, $kg.s^{-1}.m^{-2}$
$m_{\rho frost}$ – mass flux of CO_2 from the gas phase contributing to densification of frost inner layers, $kg.s^{-1}.m^{-2}$
$m_{\rho frost,surf}$ – mass flux of CO_2 at interface frost-gas contributing to densification of frost inner layers, $kg.s^{-1}.m^{-2}$
$m_{\rho fr}$ – mass flux densifying frost layers, $kg.s^{-1}.m^{-2}$
$m_{\theta fr}$ – mass flux contributing to thickness growth, $kg.s^{-1}.m^{-2}$
m – mass flow, kg/h
P – pressure of gas, bar
$Q_{conduction}$ – heat flux driven by conduction through the frost layers, $kW.m^{-2}$
$Q_{cond,surf}$ – conductive heat flux at surface, $kW.m^{-2}$
Q_{lat} – heat flux of latent heat of condensation, $kW.m^{-2}$
$Q_{lat,surf}$ – latent heat flux at gas-frost interface, $kW.m^{-2}$
Q_{sens} – sensible heat flux, $kW.m^{-2}$
$Q_{sens,surf}$ – sensible heat flux at the interface gas-frost, $kW.m^{-2}$
$Q_{tot,surf}$ – total heat flux at gas-frost interface, $kW.m^{-2}$
Q_y – heat flux in position y, $kW.m^{-2}$
Q_{y+dy} – heat flux in position y + dy, $kW.m^{-2}$
T – temperature, C
T_{biogas} – temperature of biogas bulk, C
T_{fr} – temperature gradient in frost layers, C
$T_{fr,surf}$ – temperature of interface gas-frost layer, C
$T_{surface}$ – temperature of surface, C
T_y – temperature in position y, C
$x_{CO2/CH4}$ – mass fraction of CO_2 in CH_4, $kg.kg^{-1}$
$x_{CO2,y}$ – CO_2 concentration in position y, $kg.kg^{-1}$
$x_{fr,surf}$ – mass fraction at frost – gas interface, $kg.kg^{-1}$
x, y – cartesian coordinates
ρ_{biogas} – density of biogas, $kg.m^{-3}$
ρ_{frost} – density of frost bulk, $kg.m^{-3}$

Acknowledgements

This work has been supported by the CARNOT MINES Institute within the aim of exploring new processes for biomass utilisation.

References

Chaemchuen S., Kabir N.A., Zhou K., Verpoort F., 2013, Metal–organic frameworks for upgrading biogas via CO_2 adsorption to biogas green energy, Chemical Society Reviews, 42(24), 9304, DOI: 10.1039/c3cs60244c.

Clodic D., Younes M., 2003, A new Method for CO_2 Capture - Frosting CO_2 at Atmospheric Pressure, 6th International Conference Greenhouse Gas Control Technologies, vol. I, Elsevier, 155–160.

Haddad S., 2019, Controlled Solid-Vapour CO_2 phase transitions in methane rich streams applied to biogas upgrading. PhD thesis, MINES Paristech, France.

He-Sheng R., 2004, Construction of a generalized psychrometric chart for different pressures, International Journal of Mechanical Engineering Education, 32(3), 212-222, DOI:10.7227/IJMEE.32.3.3.

Kadam R., Panwar N.L., 2017, Recent advancement in biogas enrichment and its applications, Renewable and Sustainable Energy Reviews, 73, 892–903, DOI: 10.1016/j.rser.2017.01.167.

Lee K.S., Kim W.S., Lee T.H., 1997, A one-dimensional model for frost formation on a cold flat surface, International Journal of Heat and Mass Transfer, 40(18), 4359–4365, DOI:10.1016/S0017-9310(97)00074-4.

Martin R., Murach L., 2012, Worldwide power generation from biogas will double by 2022, Businesswire, PikeResearch, USA.

MRR, 2018, Global Biogas Plant Market Professional Survey Report 2019, Market Research reports, ID PB510194233, USA.

Song C.F., Kitamura Y., Li S.H., 2012, Evaluation of Stirling cooler system for cryogenic CO_2 capture, Applied Energy, 98, 491–501, DOI: 10.1016/j.apenergy.2012.04.013.

Tuinier M.J., van Sint Annaland M., Kuipers J.A.M., 2011, A novel process for cryogenic CO_2 capture using dynamically operated packed beds—An experimental and numerical study, International Journal of Greenhouse Gas Control, 5(4), 694–701, DOI: 10.1016/j.ijggc.2010.11.011.

Wilken D., Strippel F., Hofmann F., Maciejczyk M., Klinkmuller L., Wagner L., Bontempo G., Munich J., Scheidi S., Conton M., Deremince B., Walter R., Zetsche N., Findersen C., 2017, Biogas to biomethane, Fachverband Biogas e.V, ISBN 5510-487X, UNIDO

Xu G., Li L., Yang Y., Tian L., Liu T., Zhang K., 2012, A novel CO_2 cryogenic liquefaction and separation system, Energy, 42(1), 522–529, DOI: 10.1016/j.energy.2012.02.048.